

Controllability of Wavepacket Dynamics in Coherently Driven Double-Well Potential

Akira Igarashi*

*Graduate School of Science and Technology, Niigata University,
Ikarashi 2-Nochou 8050, Niigata 950-2181, Japan*

Hiroaki Yamada†

YPRL, 5-7-14 Aoyama, Niigata 950-2002, Japan

(Dated: April 30, 2018)

We numerically study controllability of quantum dynamics in a perturbed one-dimensional double-well potential by using an optimal control theory. When the perturbation strength is small the dynamics of an initially localized Gaussian wavepacket shows coherent oscillation between the wells. It is found that as the increase of the strength and/or the number of frequency components of the perturbation the coherent motion of the Gaussian wavepacket changes to an irregular one with irreversible delocalization. We investigate the controllability of the system depending on the perturbation parameters and the initial quantum state by focusing mainly on the delocalized state generated by the polychromatical perturbation. In relatively long-time control for the Gaussian wavepacket and the delocalized state, we show that it is well-controllable via the first excited state doublet in spite of the perturbation parameters. On the other hand, in the relatively short-time control we show difficulty of the control for the delocalized state because of the numerous local minima. Furthermore, it is demonstrated that chaotic phase space structure of the system assists the controllability of the delocalized state.

PACS numbers: 05.45.M+, 05.45.Gg, 66.35.+a

I. INTRODUCTION

Decoherence of the quantum dynamics and a control of the wavepacket dynamics by using an external force field are recent attractive topics. There are many studies on environment-induced quantum decoherence by coupling the quantum system to a reservoir [1, 2, 3, 4]. Quantum dissipation due to the interaction with chaotic degrees of freedom has been also studied [5, 6, 7]. It is expected that the quantum dynamics is sensitive to any disruption of coherence as it occurs due to an unavoidable coupling to the environment. One of obstacles for experimental realization of a quantum computer is decoherence of a quantum state caused by coupling to the other degrees of freedom [8].

On the other hand, in the experimental realization of control of the chemical reactions and the optical molecular devices, a design of the control field based on optimal control theory (OCT), is also an important topic [9, 10, 11, 12, 13]. Recently, some methods to control the transition between quantum states have been proposed [14, 15, 16, 17, 18, 19, 20, 21, 22]. Our main interest is in the controllability between the quantum states in, what we call, a quantum chaos system [23, 24].

In the previous papers [25, 26], we investigated influence of chaos on quantum tunneling and decoherence in a parametrically driven double-well system modeled by

the following Hamiltonian,

$$H_0(t) = \frac{p^2}{2} + \frac{q^4}{4} - A(t)\frac{q^2}{2}, \quad (1)$$

$$A(t) = a - \frac{\epsilon}{\sqrt{M}} \sum_{i=1}^M \sin(\Omega_i t), \quad (2)$$

where q and p represent the generalized coordinate and the conjugate momentum, respectively. Here M denotes the number of mutually incommensurate frequency components $\{\Omega_i, i = 1, 2, \dots, M\}$. We choose off-resonant frequencies which are far from both classical and quantum resonance in the corresponding unperturbed case ($\epsilon = 0$). The number M of frequency components in the polychromatic oscillation corresponds to the number of degrees of freedom coupled to the unperturbed double-well system [27]. The details of relation between the time-dependent Hamiltonian and the autonomous representation have been shown in Ref.[45].

Note that in the previous works of Lin *et al.*, they dealt with a double-well system driven by single forced oscillator, therefore, the asymmetry of the potential play a role in the chaotic behavior and tunneling transition between the quasienergy states [28, 29, 30]. However, in our model the potential form is remained symmetric during the time evolution process, and different mechanism from the forced oscillation makes the classical chaotic behavior. We classified the motions of an initially localized Gaussian wavepacket depending on the perturbation parameters (M, ϵ) , i.e. *coherent motions* like an instanton and *irregular motions* of a delocalized state [26]. We call the delocalized state in the irregular motion *chaos-induced delocalized state* in this paper.

*Electronic address: f99j806b@mail.cc.niigata-u.ac.jp

†Electronic address: hyamada@uranus.dti.ne.jp

The purpose of this article is to present numerical results on the control of the quantum dynamics in the one-dimensional double-well potential with the coherent perturbation. The controllability of the system depends on the perturbation parameters and the initial state. In the relatively long-time control the displacement of the Gaussian wavepacket is well-controllable by a designed field based on OCT in the perturbed double-well potential regardless of the external parameters. Furthermore, in the relatively short-time control we show the difficulty of the control for the chaos-induced delocalized state generated under the perturbation because of numerous local optimal fields, compared to the case of Gaussian wavepacket. It is numerically demonstrated that when the system is fully chaotic by the increase of the perturbation strength ϵ the controllability of the delocalized state can be enhanced by the chaotic behavior. We call the phenomenon *chaos-assisted control* in this paper.

The remained sections of the present paper are as follows. In the next section we give some backgrounds and the numerical setting of the model and brief review of chaos-induced delocalized state. In Sect. 3 we shortly explain the optimal control theory used in the numerical calculation. In Sect. 4 we give numerical results for control between Gaussian wavepackets in the polychromatically perturbed system. In Sect. 5 we show results of the transition between a chaos-induced delocalized state and a Gaussian wavepacket. In Sect. 6 and 7 the difficulty of the control due to the local minima and the chaos-assisted control are investigated for the short-time control, respectively. The last section contains summary and discussion.

II. MODEL AND CHAOS-INDUCED DELOCALIZED STATE

In this section we give the details of the setting in the Eq.(2) and in the numerical calculation. Furthermore, we give a brief review on occurrence of a irregular motion in the delocalized state. The parameters are set as $a = 5$, $\epsilon = 0.1 \sim 1.0$, to emphasize the tunneling effect in the energetically and/or dynamically forbidden region during the time evolution. We used the following Gaussian wavepacket localized at a bottom of the right well as,

$$\psi_i(q) = (\sigma\pi)^{1/4} \exp\left\{-\frac{(q-q_0)^2}{2\sigma}\right\}, \quad (3)$$

where $q_0 = \sqrt{a}$ is the position of the right bottom and the spread of the initial packet $\sigma \sim 0.3$ as the initial state at $t = 0$. $\hbar = 1.0$ and time mesh δt is order of 10^{-2} . The spatial discretization is chosen so that $2^8 (= 256)$ points cover the interval $[-5.5, 5.5]$. The Gaussian wavepacket can be approximately generated by the linear combination of the ground state doublet as $\psi_i(q) \sim \frac{1}{\sqrt{2}}(\phi_0(q) + \phi_1(q))$, where ϕ_0 and ϕ_1 denote the

ground state doublet. (See Fig.1.) Indeed, the ammonia molecule is well described by this barrier height with two doublets with energies below the top of the barrier, and the quantum dynamics is well approximated by the several levels from the bottom of the well in the weekly perturbed case [31].

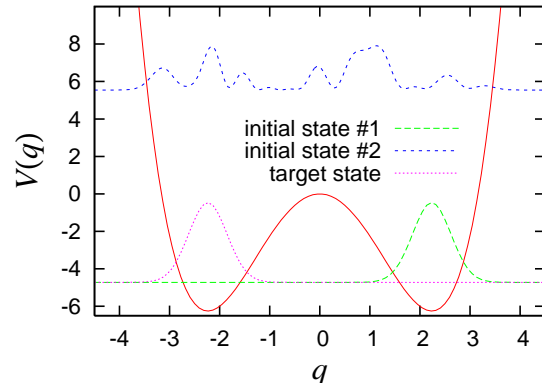


FIG. 1: The initial (target) Gaussian wave function $|\psi_i(t=0)|^2$ ($|\psi_f(t=t_f)|^2 \equiv |\Phi_f|^2$), respectively. The dotted line shows a delocalized state as the initial state, which is generated by time-evolution ($t = 5.54 \times 10^3$) in the perturbed case ($M = 10$, $\epsilon = 1.0$). The curve of the double-well potential is also plotted.

In the classical dynamics, such a system shows chaotic behavior by the oscillatory force $A(t)$ [25, 26]. The Newton's equation of the motion in the monochromatically perturbed case ($M = 1$) is

$$\frac{d^2q}{dt^2} - (a - \epsilon \sin \Omega t)q + q^3 = 0. \quad (4)$$

Note that the classical system is known as nonlinear Mathieu equation which can be derived from surface acoustic wave in piezoelectric solid [32] and nanomechanical amplifier in micronscale devices [33]. In the polychromatically perturbed cases ($M > 1$) the smaller the strength ϵ can generate chaotic behavior of the classical trajectories the larger M is [26].

We define transition probability $P_L(t)$ of finding the wave packet in the left well and a *degree of coherent motion*, ΔP_L , based on the fluctuation of the transition probability as,

$$P_L(t) \equiv \int_{-\infty}^0 |\psi(q,t)|^2 dq, \quad (5)$$

$$\Delta P_L \equiv \sqrt{\langle (P_L(t) - \langle P_L(t) \rangle_T)^2 \rangle_T}, \quad (6)$$

where $\langle \dots \rangle_T$ represents time average value for a period $T (\sim 9.4 \times 10^3)$ [26]. In the cases that perturbation strength ϵ is relatively small, $P_L(t)$ can be interpreted as the tunneling probability that the initially localized wave packet goes through the central energy barrier and reaches the left well.

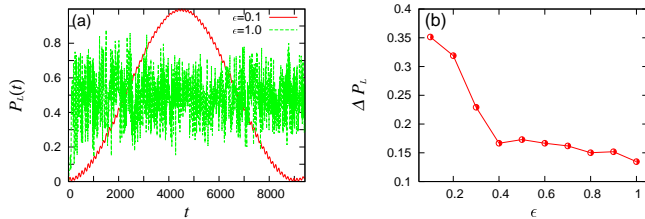


FIG. 2: (a) Transition probability $P_L(t)$ as a function of time t for $M = 10$ with $\epsilon = 0.1, 1.0$. (b) ϵ dependence of the degree of the coherent motion ΔP_L in the case.

Figure 2(a) shows the time-dependence of $P_L(t)$ in the polychromatically perturbed case ($M = 10$). Apparently we can observe two kinds of time-dependence, i.e. coherent ($\epsilon = 0.1$) and irregular ($\epsilon = 1.0$) motions. In order to estimate quantitatively the difference between coherent and irregular motions, we use the *degree of coherent motion* ΔP_L in Eq.(6) and roughly divide the types of motion of wavepacket as seen in Fig.2(b). In the *coherent motions*, the values of ΔP_L 's are almost same to the unperturbed case, i.e. $\Delta P_L \gtrsim 0.3$. In the *irregular motions* which are similar to the stochastically perturbed case, the values of ΔP_L 's becomes much smaller, i.e. $\Delta P_L \lesssim 0.2$. In the irregular motions, the wavepacket is delocalized over the both the wells as seen in Fig.1. The delocalized state cannot show the recurrence to the Gaussian shape within the accessible computation time. We call delocalized states in the irregular motions *chaos-induced delocalized state* in this paper.

It is well-known that an existence of a turning point breaks the Gaussian shape during the tunneling process even in a coherent motion. However, in the coherent motion after the tunneling process the wavepacket goes back to the Gaussian shape again. In the following sections we give numerical results of the controllability for the Gaussian wavepacket and the *chaos-induced delocalized state* corresponding to the irregular motion.

III. OPTIMAL CONTROL OF QUANTUM DYNAMICS

In this section, we briefly explain the OCT [9, 11] we used in the numerical calculation.

We consider the total Hamiltonian $H(t)$ combined the system $H_0(t)$ with the interaction by the external field $E(t)$ as,

$$H(t) = H_0(t) - \mu(q)E(t). \quad (7)$$

The second term in Eq.(7) means the interaction between the transition dipole moment $\mu(q)$ ($\equiv q$) and the external field $E(t)$, where the charge is set unity. Note that we adapted the Hamiltonian $H_0(t)$, including the time-dependent part $-A(t)\frac{q^2}{2}$, as a controlled system. However, we confirmed that if we use the static double-well

system, i.e. $\epsilon = 0$, as the controlled system the numerical result does not change in the essential point, except for one in Sect.VII where the effect of the perturbation strength is discussed.

The OCT gives an optimized external field $E(t)$ in order to produce the target state Φ_f at the target time $t = t_f$ starting from an initial state $\psi_i(t = 0)$. The objective functional $J[E(t)]$ so as to maximize is

$$J[E(t)] = |\langle \psi_i(t_f) | \Phi_f \rangle|^2 - \alpha \int_0^{t_f} E(t)^2 dt - 2\text{Re} \left[\langle \psi_i(t_f) | \Phi_f \rangle \int_0^{t_f} \langle \psi_f(t) | \frac{\partial}{\partial t} - iH(t) | \psi_i(t) \rangle dt \right] \quad (8)$$

Here $\psi_i(t)$ is a wave function driven by the optimal field $E(t)$ which has been determined by the quantum states, $\psi_i(t)$ and $\psi_f(t)$ as,

$$E(t) = \frac{\text{Im}[\langle \psi_i(t) | \psi_f(t) \rangle \langle \psi_f(t) | \mu(q) | \psi_i(t) \rangle]}{\alpha}. \quad (9)$$

$\psi_f(t)$ is an inversely evolving quantum state starting from the target state $\psi_f(t = t_f) = \Phi_f$, which can be interpreted as a Lagrange multiplier to satisfy Schrödinger equation. The second term in Eq.(8) is put to limit the resulting field intensity, where α is a penalty factor to weight the significance of the external field. The optimal field strongly depends on the initial and final states, the potential parameters and the target time t_f . Note that the existence of the optimal field has been proven for large target time and small α limit in the unperturbed case [9]. Generally, when we can optimize the transition between the energy eigenstates by a π -pulse, the target time must be at least $t_f \sim O(\hbar/\Delta E)$ to resolve the energy difference ΔE .

The relation between the controllability and chaotic behavior in quantum systems has been investigated in a context of OCT [14].

IV. CONTROLLABILITY OF THE GAUSSIAN WAVEPACKET

In this section, we give numerical results that displacement of the Gaussian wavepacket can be well controlled in the perturbed double-well potential.

A. long-time control ($t_f = 300$)

We would like to control the transition between non-stationary states. Here we take Gaussian wavepackets localized around $q = q_0$ ($q = -q_0$) as the initial(target) state, respectively. (See Fig.1.) Accordingly, in the quantum control there is no energy transfer between the initial and target states. We take the target time $t_f = 300$ that is much smaller than a tunneling time

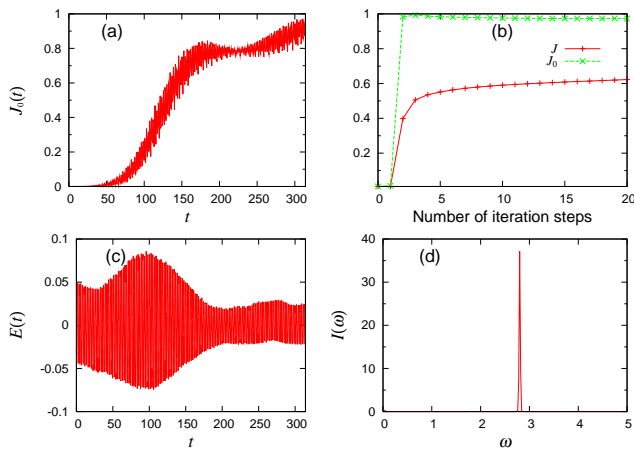


FIG. 3: Long-time optimal control of the Gaussian wavepacket in the monochromatically perturbed case ($M = 1, \epsilon = 0.1$). (a) Time-dependence of the squared final overlap $J_0(t)$ after 20 iterations. (b) Convergence of the optimized objective functional values J and J_0 as a function of the number of iteration. The panels (c) and (d) show the optimized fields $E(t)$ and the power spectrum $I(\omega)$ of the field. We used $\alpha = 1.0$ and $t_f = 300$ in the calculation.

scale $T \equiv \hbar/\Delta E_{12} \sim 9.7 \times 10^4$ in the unperturbed case ($\epsilon = 0$).

Figure 3(a) shows the final overlap $J_0(t) \equiv |\langle \psi_i(t) | \Phi_f \rangle|^2$ after 20 iterations in the monochromatically perturbed case ($M = 1$) for the target time $t_f = 300$. As we can expect, based on the OCT, the iteration of the J_0 shows fast convergence [?]. The final state by the optimal field is well overlapped for the target Gaussian function. In Fig.3(c) and (d), time dependence of the optimized field and the power spectrum are shown. The main peak of the power spectrum corresponds to energy difference between the ground state and first excited state doublets that energy is lower than the barrier height. We can immediately confirm that the wavepacket travels between the wells via the first excited state doublet by calculating some quantum mechanical mean values, $\langle H \rangle, \langle q \rangle, \langle p \rangle$, and so on during the time-evolution process.

Figure 4 shows the relatively long-time optimal control for the displacement of the Gaussian wavepacket in the polychromatically perturbed cases ($M = 10$). The function form of the optimal field depends on the extent of the chaotic behavior in the classical system. In the strongly chaotic case ($\epsilon = 1.0$) where the perturbation strength is large, the optimized field becomes a complicated function of time with many modes. The peak structure of the power spectrum shows that a lot of modes are necessary to shift the Gaussian wave packet in the strongly chaotic cases.

As a result, for the relatively long-time control between the Gaussian wavepackets with no energy deference it is almost perfectly controlled ($J_0(t_f) \sim 1.0$) regardless of the perturbation type.

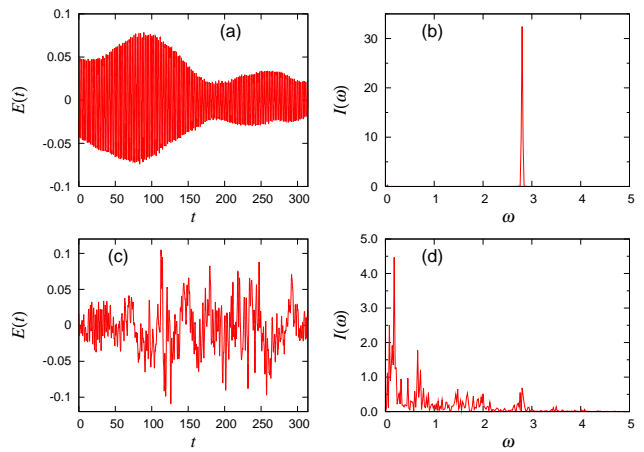


FIG. 4: Long-time optimal control of the Gaussian wavepacket in the polychromatically perturbed case ($M = 10$). (a) and (c) are the optimal fields after 20 iterations for $\epsilon = 0.1$ and $\epsilon = 1.0$, respectively. (b) and (d) are the power spectra for $\epsilon = 0.1$ and $\epsilon = 1.0$, respectively. We used $\alpha = 1.0$ and $t_f = 300$ in the calculation. $J_0(t_f) \sim 1.0$ in the both cases.

B. short-time control ($t_f = 30$)

In this subsection we also consider the control problem between the Gaussian wavepackets in the relatively short-target-time $t_f = 30$. It can be expected that the optimal field has much different function form from the π -pulse type for the short target time t_f , and that the local minima may cause instability of the convergence to the global optimal field.

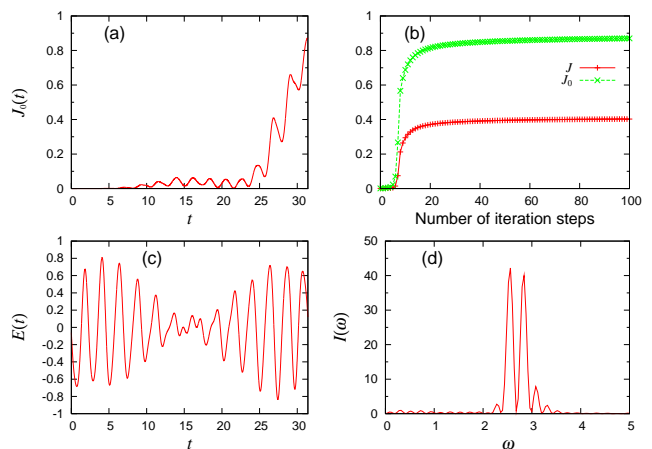


FIG. 5: Short-time optimal control of the Gaussian wavepacket in the monochromatically perturbed case ($M = 1, \epsilon = 0.1$). (a) Time-dependence of the squared final overlap $J_0(t)$ after 100 iterations. (b) Convergence of the optimized objective functional values J and J_0 as a function of the number of iteration. The panels (c) and (d) show the optimized field $E(t)$ and the power spectrum $I(\omega)$ of the field, respectively. We used $\alpha = 0.1$ and $t_f = 30$ in the calculations. $J_0(t_f) \sim 0.9$ after 100 iterations.

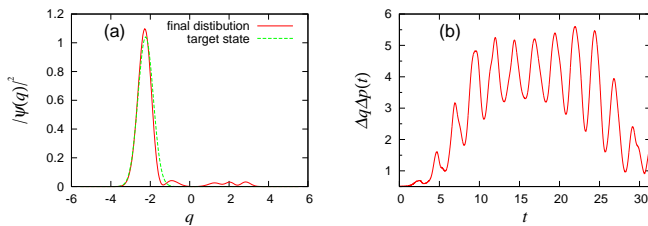


FIG. 6: (a) The probability density of the target Gaussian wavepacket and the final wavepacket achieved by using the optimal field in Fig.5(c). (b) The time-dependence of the uncertainty product $\Delta p \Delta q$ during the time-evolution by the optimal field.

In Fig.5 we show the result of the short-time optimal control in the monochromatically perturbed case ($M = 1, \epsilon = 0.1$). By adjusting the penalty parameter α for the optimization the optimal field can be almost found out even for the short-time control ($J_0(t_f) \sim 0.9$).

However, as seen in Fig.6(a) the final wavepacket has uncontrollable tail even after many iterations. The short-time optimal control is much harder than the relatively long-time ones. Figure 6(b) shows the time-dependence of the uncertainty product $\Delta p \Delta q \equiv \sqrt{\langle (q - \langle q \rangle)^2 \rangle} \sqrt{\langle (p - \langle p \rangle)^2 \rangle}$, during the time evolution by the optimal field in Fig.5(c), where $\langle \dots \rangle$ denotes quantum mechanical average. We use uncertainty product as a simple measure for quantum fluctuation in the phase space. It is found that the Gaussian wavepacket does not delocalize during the process. Furthermore, we have confirmed that the similar optimal short-time control can be achieved for the other cases with different perturbation parameters ($M = 10, \epsilon = 0.1$), ($M = 10, \epsilon = 1.0$), and so on. Here, we used $\alpha = 0.1$ to adjust the strength of the external field $E(t)$. The small value of the penalty factor allows the optimized field with the large amplitude. The existence of a lot of different optimized fields depending on α means the existence of a lot of local minima in the solution space. The details of the α -dependence will be given elsewhere [46].

Generally speaking, the non-stationary state $\Psi(t)$ at time t can be expressed by a set of the expansion coefficients $\{c_j\}_t$ as $\Psi(t) = \sum_j c_j(t) \phi_j$, where $\{\phi_j\}$ are eigen states in the unperturbed case. Accordingly, the quantum control from the initial state at $t = 0$ to the final state at $t = t_f$ is a problem to answer a question that how we can get the set of the coefficients $\{c_j\}_{t=t_f}$ in $\Phi_f = \sum_j c_j(t = t_f) \phi_j$ in starting from $\{c_j\}_{t=0}$ with obeying the Schrödinger equation. We can see that the transition between the Gaussian wavepackets can be almost attained by a change of the relatively *simple phase-relation* between the states via the first excited state doublet as ($c_0(0) = 1/\sqrt{2}, c_1(0) = 1/\sqrt{2}$) \rightarrow ($c_0(t_f) = 1/\sqrt{2}, c_1(t_f) = -1/\sqrt{2}$).

V. CONTROLLABILITY OF THE DELOCALIZED STATE

In this section, we investigate the controllability of the *chaos-induced delocalized state* as the initial state $\psi_i(t = 0)$ of the optimization procedure. Note that the target state is a localized Gaussian wavepacket in the left-well as well as the last section. Hereafter, we mainly use the polychromatically perturbed case ($M = 10, \epsilon = 1.0$) as a typical controlled system $H_0(t)$, which is strongly chaotic as shown in Fig.2.

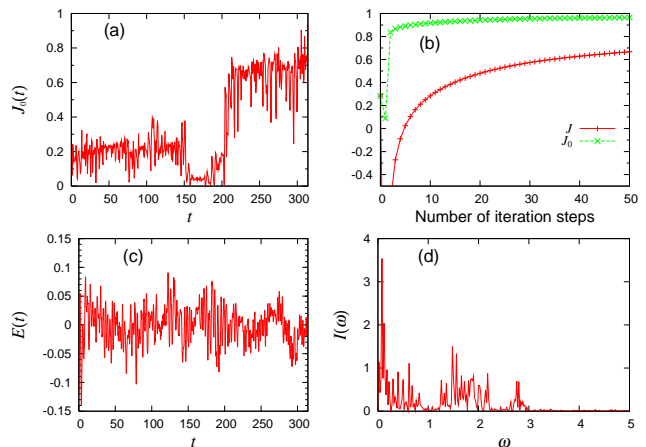


FIG. 7: Long-time optimal control for the delocalized initial state in the polychromatically perturbed case ($M = 10, \epsilon = 1.0$). (a) Time-dependence of the squared final overlap $J_0(t)$ after 50 iterations. (b) Convergence of the optimized objective functional values J and J_0 as a function of the number of iteration. The panels (c) and (d) show the optimized fields $E(t)$ and the power spectrum $I(\omega)$ of the field. We used $\alpha = 1.0$ and $t_f = 300$ in the calculation. As an initial state we used the initial delocalized state obtained by time-evolution up to $t = 5.54 \times 10^3$ in the system with $M = 10, \epsilon = 1.0$.

Figure 7 shows the relatively long-time control of the delocalized state in the polychromatically perturbed case ($M = 10, \epsilon = 1.0$). The achievement of the optimization is almost same as the case of the Gaussian wavepacket. Figure 8 shows the short-time control for the same case. It is difficult to design the optimal field for the short target-time ($t_f = 30$). As seen in Fig.8(b), it seems that the objective functional value saturates around $J_0 \sim 0.8$ even for 200 iterations, and the state is trapped in a local minimum in the optimization process. The optimized field consists of a lot of complicated modes as seen in Fig.8(d).

Figure 9(a) and (c) show the final states by using the optimized fields in Fig.8(c) and Fig.7(c), respectively. Figure 9(b) and (d) show the time-dependence of $\Delta p \Delta q$ during the time-evolution by the optimized field. Although the quantum fluctuation gradually decreases from the initial large value of the delocalized state toward small value (~ 0.5) in the final Gaussian wavepacket, it is hard to squeeze the delocalized state in the short-time

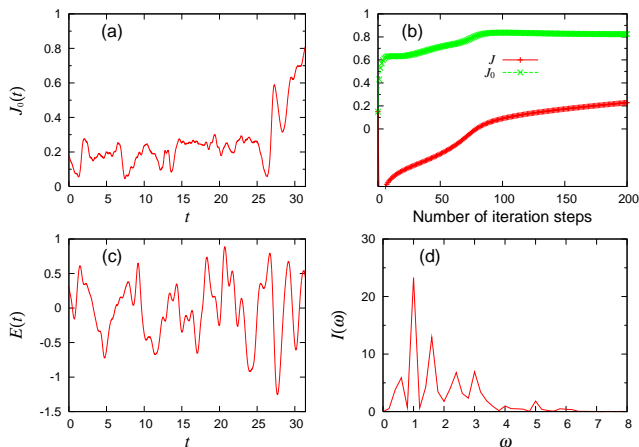


FIG. 8: Short-time optimal control for the delocalized initial state in the polychromatically perturbed case ($M = 10, \epsilon = 1.0$). (a) Time-dependence of the squared final overlap $J_0(t)$ after 200 iterations. (b) Convergence of the optimized objective functional values J and J_0 as a function of the number of iteration. The panels (c) and (d) show the optimized field $E(t)$ and the power spectrum $I(\omega)$ of the field. We used $\alpha = 0.1$ and $t_f = 30$ in the calculation. As an initial state we used the initial delocalized state obtained time-evolution up to $t = 5.54 \times 10^3$ in the system with $M = 10, \epsilon = 1.0$.

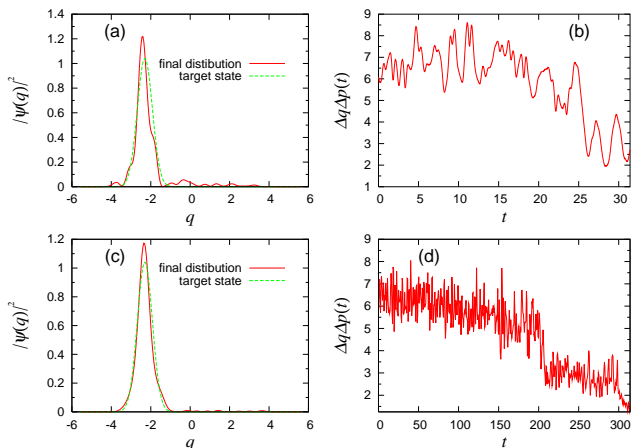


FIG. 9: (a), (c) The probability density of the target wavepacket and final wavepacket achieved by using the optimal field in Fig.8(c) and Fig.7(c), respectively. (b), (d) The time-dependence of the uncertainty product $\Delta p \Delta q$ during the time-evolution by the optimal field in Fig.8(c) and Fig.7(c), respectively.

control.

Figure 10 shows the final overlap J_0 as a function of target time t_f . The time-dependence of the functional values J_0 show irregular increase with time. It seems that the J_0 suddenly increases around $t_f = 100$ and almost saturates to $J_0 \sim 1.0$ around $t_f \sim 1000$. Apparently the longer the target time becomes the better optimization achieves. We can expect that the optimized field converges to the global minimum for the longer target

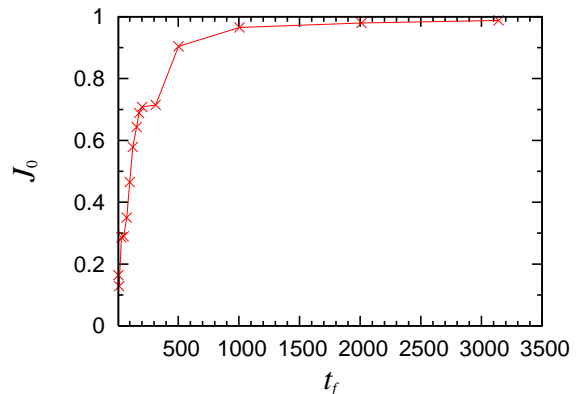


FIG. 10: t_f -dependence of the optimal control of the delocalized state in the unperturbed case. The squared final overlap $J_0(t_f)$ after 50 iterations as a function of target time t_f . We used $\alpha = 1.0$ in the all calculations. As an initial state we used the initial delocalized state obtained by time-evolution up to $t = 5.54 \times 10^3$ in the system with $M = 10, \epsilon = 1.0$.

time.

It should be emphasized that even for the long-time control the difference of the controllability between the delocalized state and the Gaussian wavepacket is the number of iterations for the convergence that represents a cost for the optimization. The chaos-induced delocalized state consists of a lot of eigenstates on the unperturbed basis due to the mixing of multilevel caused by the perturbation.

VI. LOCAL OPTIMAL FIELD

So far, we used a typical sinusoidal field $E^{trial}(t) = \sin t$ as an initial guess at the first iteration step. The final optimized field $E(t)$ does not strongly depend on the trial field for long-time control. In this section, we investigate the influence of the initial trial field $E^{trial}(t)$ on the optimal field $E(t)$ for the short-time control as in Fig.8. For that purpose, as the initial state we use the delocalized state in the polychromatically perturbed double-well potential ($M = 10, \epsilon = 1.0$). All numerical settings are same to the last section except for the first guess of the iteration.

In Fig.11 we show several optimal fields for the short-time control in the transition between the delocalized state and the Gaussian wavepacket, where we used the following trial fields as the first guess, $E_2^{trial}(t) = \sin 2.8t$, $E_3^{trial}(t) = \frac{1}{\sqrt{M}} \sum_{i=1}^M \sin(\Omega_i t)$, $E_4^{trial}(t) = f(t)$. The $f(t)$ is randomly and uniformly distributed in the range $[-1, 1]$. As shown in the right panels of Fig.11 the shape of the power spectra corresponding to the these optimal fields are quite different with respect to one another. The function form of the optimal field $E(t)$ strongly depends on the trial function form $E^{trial}(t)$ as the first guess. Figure 12 shows the convergence to the optimal fields in the

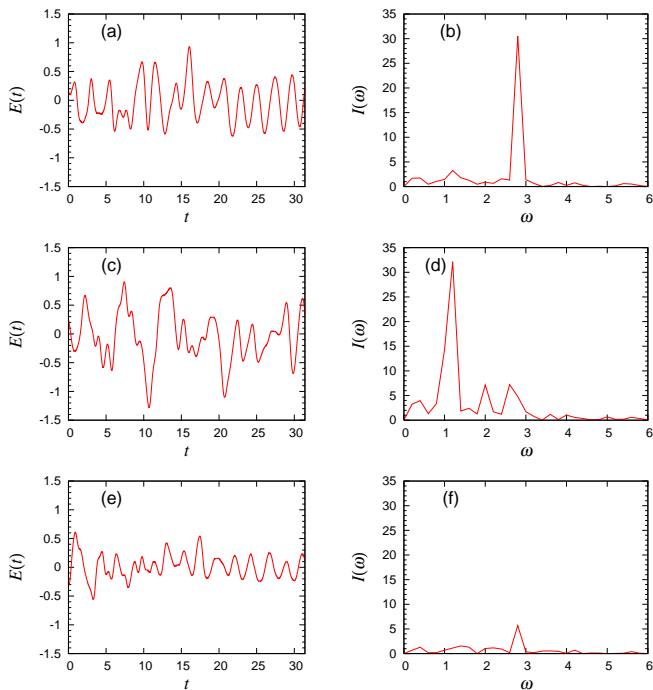


FIG. 11: The trial field $E^{trial}(t)$ dependence of the short-time control between the delocalized state and the Gaussian wavepacket in the polychromatically perturbed case ($M = 10, \epsilon = 1.0$). The left panels (a,c,e) are the optimized fields after 200 iterations for three different trial fields as the first guess, $E_2^{trial}(t)$, $E_3^{trial}(t)$ and $E_4^{trial}(t)$ given in the text. The right panels (b,d,f) are the power spectra $I(\omega)$ corresponding to the optimal fields in the left panels. We used $\alpha = 0.1$ and $t_f = 30$ in the calculation. As an initial state we used the initial delocalized state obtained (ug by) time-evolution up to $t = 5.54 \times 10^3$ in the system with $M = 10, \epsilon = 1.0$. The final overlaps are less than 0.8 in the all cases.

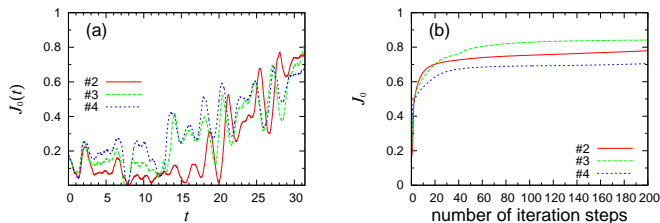


FIG. 12: Comparison with the results for the different first guesses $E^{trial}(t)$ in Fig.11. (a)Time-dependence of the squared final overlap $J_0(t)$ after 200 iterations. (b)Convergence of the optimized objective functional values J and J_0 as a function of the number of iteration. The other parameters are the same as a case in Fig.8. The curves denoted by the figures (2, 3, 4) express the results corresponding to the $E_2^{trial}(t)$, $E_3^{trial}(t)$ and $E_4^{trial}(t)$.

cases of the different initial fields $E^{trial}(t)$. The optimized values J_0 after 200 iterations are about 0.8 in all cases, and the control is incomplete.

As a result, it is conjectured that during the optimiza-

tion process the numerous local minima prevent the convergence to the global minimum corresponding to the target state. This difficulty in finding the global minimum comes from a feature of the chaos-induced delocalized state with the *complicated phase structure* like an entangled state. It is expected that the transition between the delocalized state and the Gaussian wavepacket can be achieved by the more complicated control due to existence of a lot of local minima in the solution space via the excited states with high energy than that between the Gaussian wavepackets. In the short-time control, for the sake of the manipulation of the control field for the delocalized states, we need some strategies in order to throw off the trap in the local minimum, such as genetic algorithm [34] and chaotic itinerancy [35]. Further investigation is necessary to find the global optimal field for short-time control problem concerning the chaos-induced delocalized state [46]. The development of new optimal control method is out of scope in this paper.

VII. CHAOS-ASSISTED CONTROL

In this section, we consider influence of chaos in the controlled system $H_0(t)$ on the controllability for the delocalized state. All numerical settings are same to the last section except for the first guess of the iteration except for value of ϵ in $A(t)$.

As shown in Sect.II the chaotic behavior in the perturbed double-well system is enhanced by the increase of the perturbation strength ϵ .

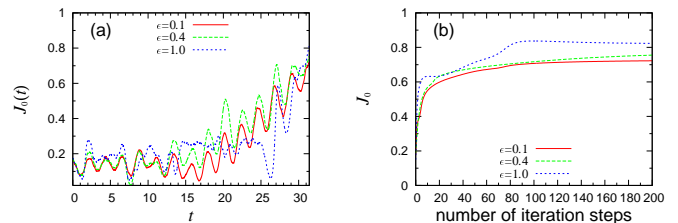


FIG. 13: ϵ -dependence of the short-time control in the polychromatically perturbed case ($M = 10$). (a)Time-dependence of the squared final overlap $J_0(t)$ after 200 iterations. (b)Convergence of the optimized objective functional value J and J_0 as a function of the number of iteration. We used $\alpha = 0.1$ and $t_f = 30$ in the calculation. As an initial state we used the delocalized state obtained time-evolution up to $t = 5.54 \times 10^3$ in the system with $M = 10, \epsilon = 1.0$.

Figure 13 shows the short-time control for various values of ϵ ($= 0.1, 0.4, 1.0$) in the polychromatically perturbed case ($M = 10$). It found that the controllability is suppressed and the final overlap less converges to the target state as the decrease of the perturbation strength. We can regard that the strong chaotic mixing in the double-well system assists the control of the transition between the quantum states. We call the phenomenon *chaos-assisted control*.

A simple scenario for chaos-assisted control is attributed to the following fact. In a weak chaotic system with small perturbation strength, the existence of the dynamical structure in the phase space can work as the obstacles for the motion of the wavepacket. On the other hand, the strong perturbation can remove the restriction of the motion and make displacement of the wavepacket smoother than the weakly perturbed case. The chaos-assisted control can be also observed in short-time control between Gaussian wavepackets discussed in the last section.

What cases are uncontrollable even for long-target-time t_f ? The energy difference between the initial and target states may make difficult to control the transition of the delocalized state if the initial state is at least a non-stationary state with high energy. We have confirmed the difficulty of the control even for a very long-target time optimization when we use a delocalized state with the higher energy as an initial state. Then, it can be expected that the harder the control becomes the more efficient the chaos-assisted control may work, although the control is still far from the perfect one. The details will be reported elsewhere in focusing on the more systematic investigation for this point [46].

VIII. SUMMARY AND DISCUSSION

In summary, we numerically investigated controllability of the wave packet dynamics in the polychromatically perturbed one-dimensional double-well system based on the optimal control theory. The controllability depends on the target time t_f and the initial state. The results are summarized as follows.

(1) In the cases of the relatively long-time control for the displacement between the localized Gaussian wavepackets in the wells, it can be well-controllable regardless of the perturbation type.

(2) In the cases of the relatively short-time control for the Gaussian wavepackets, we can obtain the almost optimal field although the convergence of the iteration is slowly.

(3) When we use a delocalized state as the initial state, which is obtained by the time-evolution under the polychromatic perturbation ($M = 10, \epsilon = 1.0$), the quantum control becomes more insufficient than the case of the Gaussian wavepacket. The convergence of the iteration is slow because of numerous local minima.

(4) As the increase of the perturbation strength ϵ in the controlled system the controllability of the delocalized state can be enhanced because the restriction caused by the dynamical structure could be broken in the fully

chaotic state.. We called the phenomenon *chaos-assisted control*.

It is interesting that whether or not the short-time optimization of the delocalized state is well-controllable by the other control methods, for example, noniterative method and so on, proposed by some groups [14, 16].

We modeled the other degrees of freedom coupled with the double-well system as external coherent perturbation in Eq.(1). A control problem for a quantum system interacting with a bath composed of finite (or infinite) degrees of freedom is interesting [19, 22]. The application of OCT to laser driven hydrogen tunneling by using ultrafast laser pulses have been proposed by some groups [36]. Then decoherence through coupling to intermolecular and intramolecular degrees of freedom is inevitable in the realistic system. The influence of the other degrees of freedom is modeled as coupling with an infinite collection of harmonic oscillators characterized by a broad and continuous distribution of frequencies. From the point of view, we modeled the effect of coupling with the other degrees of freedom as a coupling with finite collection of highly excited harmonic oscillators with some discrete special frequencies. The control of the dissipative quantum state and entangled state are directly related to the realization of the quantum computation [37, 38].

The transfer mechanism of the well-localized Gaussian wavepacket between the wells has an analogy with Mott's variable range hopping (VRH) between the localized states in (ig a) disordered system containing the roughness in the potential energy landscape, which is a dominant transport mechanism in low-temperature limit [39]. On the other hand, the conductive properties of DNA have recently attracted interest [40, 41, 42, 43]. The lambda phase DNA (λ -DNA) has been sometimes modeled as a one-dimensional disordered system, and there has been an explanation for the electrical conductivity along the DNA double helix, by using the VRH based on the temperature dependence of the conductivity [44]. Therefore, the control of the electron transfer in the disordered system composed of fluctuating multi-well potential is also interesting problem.

Moreover, we can realize the another delocalized state in the polychromatically perturbed one-dimensional disordered system [45]. The more details of the controllability of the delocalized states in the disordered system and the double-well system will be reported in the future [46].

The authors would like to thank Prof. K.S. Ikeda and Prof. M. Goda for encouragements and interests in this study. We also would like to thank Dr. T. Takami for useful discussion in some meetings.

[1] A.O. Caldeira and A.J. Leggett, Phys. Rev. Lett. **46**, 211(1981).

[2] U. Weiss, *Quantum Dissipative Systems, second edition* (World Scientific, 1999).

- [3] T. Dittrich and R. Graham, Z. Phys. B 62, 515(1986); Ann. Phys. **200**, 363(1990).
- [4] D. Cohen, Phys. Rev. Lett. **82**, 4951(1999).
- [5] W.H. Zurek and J.P. Paz, Phys. Rev. Lett. **72**, 2508(1994); S. Habib, *et al.*, Phys. Rev. Lett. **88**, 040402(2002).
- [6] A.R. Kolovsky, S. Miyazaki, and R. Graham, Phys. Rev. E **49**, 70(1994).
- [7] I. Percival, *Quantum State Diffusion* (Cambridge Univ. press 1998).
- [8] M.A. Nielsen and I.L. Chuang, *Quantum Computation and Quantum Information*, (Cambridge Univ. Press, 2000).
- [9] S.A. Rice and M. Zhao, *Optical Control of Molecular Dynamics* (Wiley Interscience Publication, 2000).
- [10] M. Shapiro and P. Brumer, *Principles of the Quantum Control of Molecular Processes* (Wiley Interscience Publication, 2003).
- [11] W. Zhu, J. Botina and H. Rabitz, J. Chem. Phys. **108**, 1953(1998).
- [12] H. Umeda and Y. Fujimura, Chem. Phys. **274**, 231(2001).
- [13] Y. Ohta, T. Yoshimoto and K. Nishikawa, Chem. Phys. Lett. **316**, 551(2000).
- [14] T. Takami, H. Fujisaki and T. Miyadera, Adv. Chem. Phys. **130A**, 435(2005).
- [15] B.K. Dey, J. Phys. A **33**, 4643(2000).
- [16] E. Dennis and H. Rabitz, Phys. Rev. **A67**, 033401(2003).
- [17] K. Bergmann, H. Theuer and B.W. Shore, Rev. Mod. Phys. **70**, 1003(1998).
- [18] C. Zhu, Y. Treaishi and H. Nakamura, Adv. Chem. Phys. **117**, 127-233 (2001).
- [19] S.G. Schirmer, Phys. Rev. **A63**, 013407(2000).
- [20] L.E. deAraujo and I.A. Walmsley, J. Opt. B: Quantum Semiclass. **5**, R27(2003).
- [21] M. Sugawara, Chem. Phys. Lett. **378**, 603(2003).
- [22] D. D'Alessandro and M. Dahleh, *Proceedings of the 41st IEEE Conference on Decision and Control*, p40(2002).
- [23] M. Gutzwiller, *Chaos in Classical and Quantum Mechanics* (Springer, Berlin, 1990).
- [24] F. Haake, *Quantum Signatures of Chaos* (Springer, Berlin, 2001).
- [25] A. Igarashi and H. Yamada, Chem. Phys. **309**, 95(2005).
- [26] A. Igarashi and H. Yamada, preprint, cond-mat/0508483.
- [27] The details of the correspondence has been given in [45].
- [28] W.A. Lin and L.E. Ballentine, Phys. Rev. Lett. **65**, 2927(1990); Phys. Rev. A **45**, 3637(1992).
- [29] F. Grossmann, T. Dittrich, P. Jung and P. Hänggi, Phys. Rev. Lett. **67**, 516(1991); M. Grifoni and P. Hänggi, Phys. Rep. **304**, 229(1998).
- [30] L. Gammaioni, P. Hänggi, P. Jung and F. Marchesoni, Rev. Mod. Phys. **70**, 223(1998).
- [31] V. Delgado and J.M.G. Llorente, Phys. Rev. Lett. **88**, 053603(2002).
- [32] H. Konno, J. Phys. Soc. Jpn. **59**, 3989(1990).
- [33] D.A. Harrington and M.L. Roukes, preprint(2002).
- [34] M. Sugawara, Comput. Phys. Commun., **140**, 366(2001); M. Sugawara, M. Yamanouchi, and S. Yabushita, Chem. Phys. Lett. **396**, 136(2004).
- [35] K. Kaneko, Physica D **41**, 137(1990).
- [36] H. Naundorf, K. Sundermann and O. Kuhn, Chem. Phys. **240**, 163 (1999); E. Geva, J. Chem. Phys. **116**, 1629(2002).
- [37] R.P. Feynman, *Feynman Lectures on Computation* (Perseus Books Group 1996).
- [38] S. Kawabata, Phys. Rev. A **68**, 064302(2003).
- [39] N. F. Mott and E. A. Davis, *Electronic Processes in Non-Crystalline Solids* (Oxford University, London, 1971).
- [40] R.G. Endres, D.L. Cox and R.R.P. Singh, Rev. Mod. Phys. **76**, 195(2004).
- [41] S. Roche and E. Macia, Mod. Phys. Lett. B **18**, 847(2004).
- [42] D. Klotsa, R.A. Roemer and M.S. Turner, Biophys. J. **89**, 2187(2005).
- [43] R. Gutierrez, S. Mandal and G. Cuniberti, Nano Lett. **5**, 1093(2005).
- [44] Z. G. Yu and Xueyu Song, Phys. Rev. Lett. **86**, 6018(2001).
- [45] H. Yamada and K.S. Ikeda, Phys. Rev. E **59**, 5214(1999); *ibid*, **65**, 046211(2002).
- [46] A. Igarashi and H. Yamada, in preparation.